Spin fluctuations in superconducting $La_{1.85}Sr_{0.15}CuO_4$

M. Matsuda,* K. Yamada, and Y. Endoh
Department of Physics, Tohoku University, Sendai 980, Japan

T. R. Thurston and G. Shirane
Department of Physics, Brookhaven National Laboratory, Upton, New York 11973

R. J. Birgeneau and M. A. Kastner
Department of Physics, Massachusetts Institute of Technology, Cambridge, Massachusetts 02139

I. Tanaka and H. Kojima
Institute of Inorganic Synthesis, Faculty of Engineering, Yamanashi University, Kofu 400, Japan
(Received 20 July 1993)

Neutron-scattering experiments have been performed to study the dynamic spin properties of $La_{1.85}Sr_{0.15}CuO_4$ ($T_c=33$ K) in the temperature range 1.9 K $\leq T \leq$ 150 K and energy range 1.5 meV $\leq \omega \leq$ 20 meV; these span, respectively, T_c and the weak-coupling BCS gap energy $2\Delta \sim 10$ meV. The width of $S(\mathbf{q},\omega)$ in momentum space decreases with decreasing temperature at fixed energy as well as with decreasing energy at fixed T, becoming very sharp at both low ω and low temperature. It is found that both in the normal state at $T=35$ K and in the superconducting state at $T=10$ K the integrated generalized susceptibility $\chi''(\omega)=\int_{(\pi,\pi)} dq_{2D}\chi''(\mathbf{q},\omega)$ is constant above $\omega \sim 10$ meV with an amplitude about three times that in $La_{1.98}Sr_{0.02}CuO_4$ and begins to decrease with decreasing ω at $\omega \sim 10$ meV, which corresponds to the BCS superconducting gap energy 2Δ. However, we observe nonzero magnetic scattering well below the pseudogap energy at temperatures as low as 2 K. These results are compared with those in $La_{1.98}Sr_{0.02}CuO_4$ and $YBa_2Cu_3O_{6.6}$.

I. INTRODUCTION

Following the initial discovery[1] of antiferromagnetic spin fluctuations in the superconducting lamellar copper oxides, extensive experimental and theoretical studies have been carried out in order to clarify the relationship between these antiferromagnetic spin fluctuations and the superconductivity.[1-22] A series of inelastic neutron-scattering measurements (Refs. 1, 3–10, and 19–22) elucidated the dynamics of the short-range antiferromagnetic spin correlations in $La_{2-x}Sr_xCuO_4$ and $YBa_2Cu_3O_{6+x}$. In superconducting $La_{2-x}Sr_xCuO_4$ incommensurate structure in the spin fluctuations has been reported by several authors.[2-4] Recent measurements[5,6,10] have shown that the incommensurate magnetic rods are located at the reciprocal space positions $[\pi(1\pm\delta),\pi]$ and $[\pi,\pi(1\pm\delta)]$ (square lattice notation, unit lattice constant) with $\delta \sim 0.2$. The dependence of δ on x is reported in Ref. 19. The width of the rods in momentum space decreases dramatically at low energies and low temperatures.[6,10] The intensity at the $[\pi(1-\delta),\pi]$ position shows a well-defined peak at T_c at the lowest energies[6,10] thence confirming the coupling between the magnetism and the superconductivity. On the other hand, the intensity decreases monotonically with increasing temperature at higher energies.[10] This temperature dependence of $S(\mathbf{q},\omega)$ is similar to that observed by Sternlieb *et al.*[8] in $YBa_2Cu_3O_{6.6}$ ($T_c=53$ K) albeit with the energy scale reduced by a factor which is of order the ratio of the T_c's. As we shall see, the energy dependence of $S(\mathbf{q},\omega)$ in the two materials is also quite similar. This suggests that the superconductivity has the same basic character in the 2:1:4 and "plateau region" 1:2:3 systems. Theoretical calculations[11,12] using a variety of microscopic descriptions, all based on a Fermi-liquid (or "marginal"-Fermi-liquid) picture, predict both the incommensurate geometry and the temperature dependence of $S(\mathbf{q},\omega)$.

In this paper we extend our previous inelastic neutron-scattering study[10] to lower temperatures and higher energies. We have performed detailed measurements of the incommensurate scattering as a function of temperature (1.9 K $\leq T \leq$ 150 K) and energy (1.5 meV $\leq \omega \leq$ 20 meV). We also have carried out a quantitative analysis of the peak integrated intensities and widths. The superconducting transition temperature is $T_c=33$ K so that the weak-coupling BCS gap in this material is $2\Delta=3.5kT_c=10$ meV, accordingly, the temperature and energy range of the measurements span the values of interest for superconductivity. The new data and analysis reported here enable us to compare the results with, for instance, those of $YBa_2Cu_3O_{6+x}$ as well with the lightly doped material $La_{1.98}Sr_{0.2}CuO_4$ where the spin-fluctuation scattering is commensurate.

The format of this paper is as follows: Experimental details are described in Sec. II. The experimental results are presented in Sec. III. In Sec. IV we discuss the results and compare them with those of $La_{1.98}Sr_{0.02}CuO_4$ and $YBa_2Cu_3O_{6.6}$.[7,8]

II. EXPERIMENTAL DETAILS

The two single crystals of $La_{1.85}Sr_{0.15}CuO_4$ used in this experiment were grown using the traveling solvent floating-zone method.[13] One of these crystals, labeled KOS-1, has been well characterized[4] by transport and neutron-scattering measurements which show its excellent homogeneity. For the current experiments, a second sample, KOS-2, of similar quality to KOS-1, was mounted and aligned beside KOS-1 in order to increase the scattering intensity. The total crystal volume was then ~ 1 cm^3, and the combined mosacity was less than 0.3° full width at half maximum as determined by neutron diffraction. KOS-1 and KOS-2 have identical transport and magnetic properties. The combined crystals exhibit a sharp tetragonal-orthorhombic structure transition at ~ 200 K. From the sharpness of the transition we conclude that the Sr and O concentrations are uniform over the two crystals.

The inelastic neutron-scattering experiments were carried out on the three-axis spectrometer H7 at the Brookhaven High-Flux Beam Reactor. For most of the experiments the horizontal collimator sequence was $40'-80'-S-80'-80'$. The incident neutron energy was fixed at 14.7 meV for the lower energy ($\omega \leq 4$ meV) experiments, while the final neutron energy was fixed at 14.7 meV for the higher energy ($\omega \geq 5$ meV) experiments. Pyrolytic graphite single crystals were used as monochromator and analyzer; contamination from higher-order reflections was effectively eliminated using a pyrolytic graphite filter. The sample was placed in a closed-cycle refrigerator for the experiments above $T=10$ K and in a helium pumped cryostat for temperatures 1.9 K $\leq T \leq 7$ K.

In order to compare the results of measurements in $La_{1.85}Sr_{0.15}CuO_4$ with those obtained for a low Sr concentration sample, we used a crystal of $La_{1.98}Sr_{0.02}CuO_4$ which was grown from a nonstoichiometric CuO-rich solution. The crystal had just enough Sr to destroy three-dimensional long-range magnetic order and induce spin-glass behavior at low temperatures. The detailed properties of this sample are described elsewhere.[14] We performed inelastic neutron measurements on the $La_{1.98}Sr_{0.02}CuO_4$ sample utilizing the same spectrometer configurations as those described above for the $La_{1.85}Sr_{0.15}CuO_4$ measurements.

In this paper, we use the crystallographic notation pertaining to the low-temperature orthorhombic space group *Bmab*; reflections in the CuO_2 planes then have Miller indices $(h,k,0)$, while $[00l]$ is the direction perpendicular to the CuO_2 planes. The room-temperature lattice parameters of the sample are $a=b=5.340$ Å and $c=13.22$ Å; at 4.5 K they are $a=5.318$ Å, $b=5.344$ Å, and $c=13.17$ Å. The small difference between a and b at low temperatures is irrelevant for all of the measurements reported here so we shall treat the material as being effectively tetragonal. For clarity we note that the rods $(1,0,l)$ and $(\frac{1}{2},\frac{1}{2},l)$ in *Bmab* notation correspond at $l=0$ to the points (π,π) and $(0,\pi)$, respectively, in the two-dimensional (2D) square lattice, unit lattice constant notation favored by theorists.

Two configurations are used in this study. In the first, the sample is oriented for scattering in the $(h,0,l)$ zone and tilted about the (0,0,1) axis by an angle ϕ, so that scans with $q_x=h\cos\phi$, $q_y=h\sin\phi$, and $q_z=l$ arbitrary are possible; we parametrize such tilt scans by the variable h. When ϕ is set at 6°, the scattering near the incommensurate peak positions, $(0.89,0.11,L)$ and $(1.11,0.11,l)$ or, equivalently, $(0.78\pi,\pi)$ and $(\pi,1.22\pi)$, can then be probed. We show this scattering configuration in Fig. 1(a). The four rods in the left-hand part of Fig. 1(a) illustrate the incommensurate magnetic rods. The ellipse represents the resolution function of the spectrometer. The solid line in the right-hand part of Fig. 1(a) illustrates a tilt scan in which the resolution function passes near the two large black circles which represent incommensurate scattering peaks. We show in Fig. 2(a) a representative inelastic scan at $\omega=3$ meV and $T=35$ K. The peak on the right side of Fig. 2(a) is smaller than the one on the left side because the tilt scan trajectory does not pass through the center of both peaks.

In the second configuration, the sample is mounted for scattering in the $(h,k,0)$ zone. In this configuration, scans with q_x and q_y arbitrary and $q_z=0$ can be performed. This allows access to the $[\pi(1\pm\delta),\pi]$ and $[\pi,\pi(1\pm\delta)]$ positions, although only $q_z=0$ is permitted. We show in Fig. 1(b) the scattering configuration and in Fig. 2(b) a representative inelastic scan at $\omega=3$ meV and $T=35$ K. Both the intensity and the signal-to-noise ratio are higher in the $(h,0,l)$ configuration than in the $(h,k,0)$ configuration.

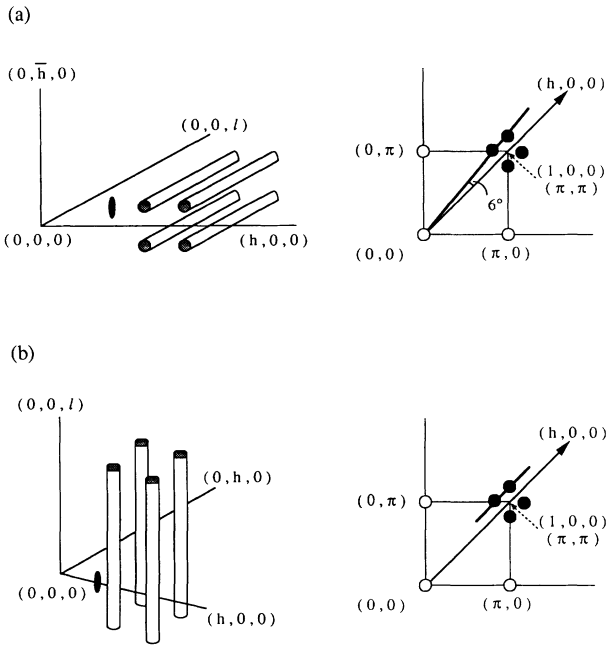

FIG. 1. The scattering configurations of the $(h,0,l)$ geometry (a) and of the $(h,k,0)$ geometry (b). The four rods and the ellipse in the left-hand figures represent the incommensurate magnetic rods and the resolution function of the spectrometer, respectively. In the right-hand figures, the solid line illustrates a scan trajectory and black circles represent incommensurate scattering peaks.

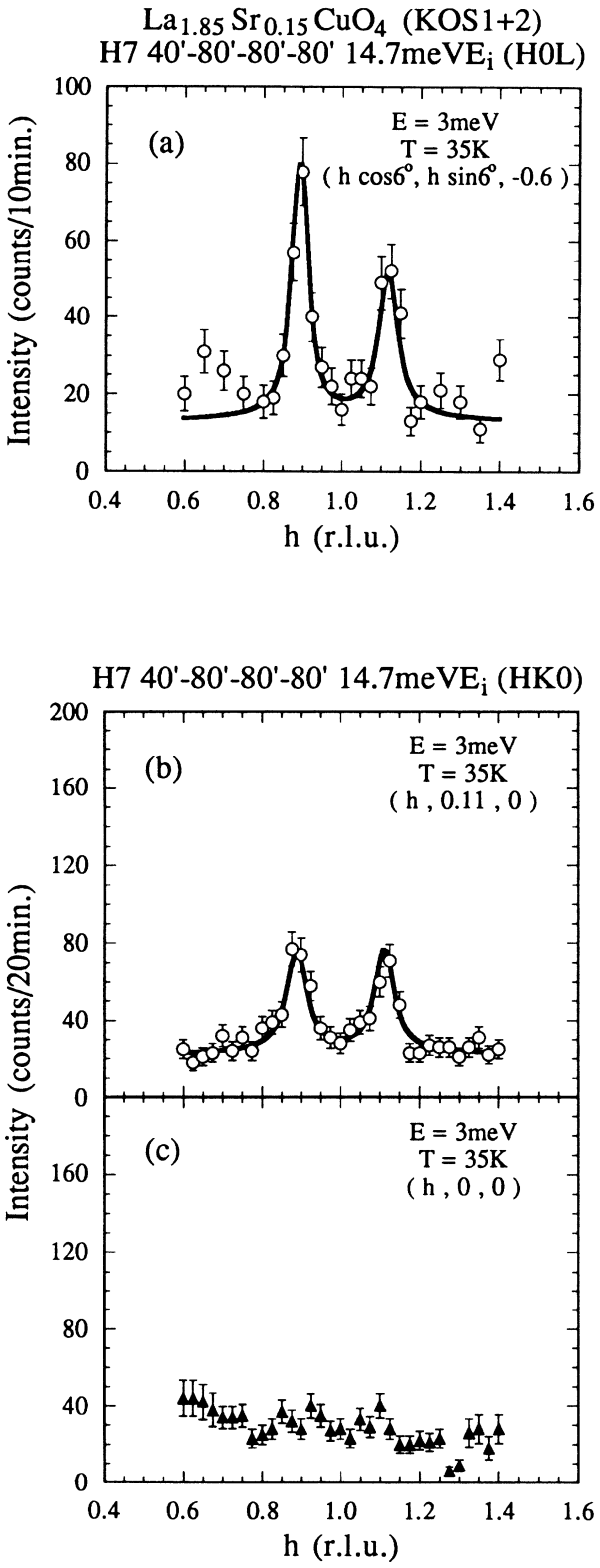

FIG. 2. Inelastic neutron-scattering spectra of $La_{1.85}Sr_{0.15}CuO_4$ at $\omega=3$ meV and $T=35$ K in the $(h,0,l)$ configuration (a) in the $(h,k,0)$ configuration (b) and through the (π,π) position in the $(h,k,0)$ configuration (c). The solid lines are from fits to four 2D isotropic Lorentzians centered at positions $[\pi(1\pm\delta),\pi]$ and $[\pi,\pi(1\pm\delta)]$ convolved with the instrumental resolution function.

Heuristically, one might expect that the observed intensity would be higher in the $(h,k,0)$ configuration than in the $(h,0,l)$ configuration due to the fact that the spectrometer vertical resolution function is elongated along the magnetic rods. Indeed, model calculations predict that the scattering intensity should be higher in the $(h,k,0)$ configuration than in the $(h,0,l)$ configuration for fine collimations. However, for the coarser collimations used in these experiments simulations predict that the scattering intensity is actually higher in the $(h,0,l)$ configuration than in the $(h,k,0)$ configuration. Furthermore, there is an advantage in using the tilt geometry in the $(h,0,l)$ configuration in that the background may be reduced considerably. This is because one can easily change l in order to minimize the background scattering from phonon and multiple-scattering processes; in addition, the tilt zone has a low symmetry so that a variety of spurious scattering processes are eliminated. In this experiment we used primarily the $(h,0,l)$ configuration with coarse collimation in order to increase both the scattering intensity and the signal-to-noise ratio.

Finally, we show in Fig. 2(c) a longitudinal scan through the (1,0,0) or equivalently, (π,π) position. As expected, the incommensurate peaks are barely visible.

III. RESULTS

We show in Fig. 3 a series of $(h,0,l)$ configuration scans at $T=1.9$ and 35 K at energies of 1.5 and 3 meV together with scans at 10 K at energies of 15 and 20 meV. The solid lines are also calculated using 2D Lorentzian profiles convolved with the instrumental resolution function. The parameters varied in these fits are the half width at half maximum (HWHM) and amplitude of the excitation together with the background which is taken as a constant for the q range probed. The splitting of the incommensurate magnetic peaks is fixed at the average value 0.0132 Å^{-1}, which has been determined from the fits of the data for 1.5 meV $\leq\omega\leq$ 8 meV where the two peaks are well resolved. The scans for $9\leq\omega\leq 20$ meV are all fitted quite satisfactorily with this fixed value; we show the results of the fits below. These data contain a number of important features. First, the excitations are remarkably sharp in momentum space at low temperatures and energies. Quantitatively similar results were obtained by Mason, Aeppli, and Mook.[6] Second, the excitation momentum width increases with increasing energy. Most importantly, from the scans at 1.9 K in Fig. 3 it is evident that these sharp, low-energy excitations persist in the superconducting state.

The intensity at the $[\pi(1-\delta),\pi]$ position has been measured as a function of temperature for temperatures 1.9 K $\leq T\leq$ 80 K and energies 1.5 meV $\leq\omega\leq$ 6 meV. Data for 10 K $\leq T\leq$ 70 K are shown as Fig. 3 in Ref. 10. We remind the reader that because of the anisotropic resolution function these data, in fact, represent one-dimensional integrations over the incommensurate peaks. As noted in Ref. 10, there is a well-defined maximum in the intensity at 1.5 and 2 meV at a temperature which to within the errors coincides with $T_c=33$ K. For $\omega=3$ and 4 meV with decreasing temperature the intensity ap-

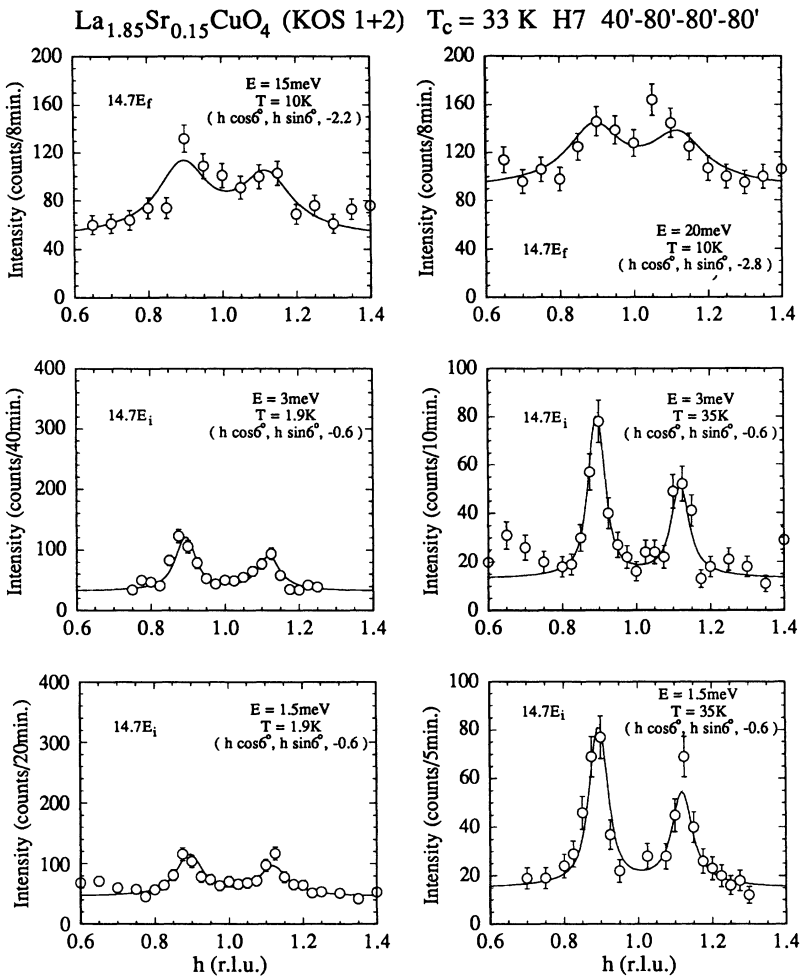

FIG. 3. Inelastic neutron-scattering spectra at $T=1.9$ and 35 K at energies of 1.5 and 3 meV together with scans at 10 K at 15 and 20 meV. All of the scans were taken in the $(h,0,l)$ configuration which has the trajectory $(h\cos 6°, h\sin 6°, l)$. Here $l=-0.6$. The lines are the results of fits to four Lorentzians centered at positions $[\pi(1\pm\delta),\pi]$ and $[\pi,\pi(1\pm\delta)]$ convolved with the instrumental resolution function as discussed in the text.

proaches a constant above T_c and then decreases by about a factor of 3 and two, respectively, between T_c and 1.9 K. However, at 6 meV there appears to be no significant effect of the superconducting transition on the amplitude of the spin fluctuations. We emphasize that the signal-to-noise ratio in these measurements is an order of magnitude better than that in previous neutron-scattering studies[1-6] of the spin fluctuations in the superconducting copper oxides and accordingly we regard these data as being correspondingly more reliable. From the intensity data one may immediately extract $\chi''(\mathbf{q},\omega)$ via the fluctuation-dissipation theorem, that is, $\chi''(\mathbf{q},\omega)=(1-e^{-\hbar\omega/kT})S(\mathbf{q},\omega)$. The results so obtained for 10 K $\leq T \leq$ 70 K are shown as Fig. 4 in Ref. 10. Above T_c, $\chi''(\mathbf{q},\omega)$ with $\mathbf{q}=[\pi(1-\delta),\pi]$ increases with decreasing temperature. To within the errors, this growth is arrested at T_c and $\chi''(\mathbf{q},\omega)$ decreases somewhat with further decrease in temperature below T_c for energies from 1.5 to 4 meV; however $\chi''(\mathbf{q},\omega)$ is approximately constant below T_c for $\omega \geq 6$ meV.

We now discuss the results extracted from fits to the individual scans. In Fig. 4 we show the HWHM as a function of temperature for 1.9 K $\leq T \leq$ 150 K and energies 1.5 meV $\leq \omega \leq$ 20 meV. Note that the quality of the data becomes worse for $\omega \leq 4$ meV and $T \geq 50$ K because of the lower intensity and the higher background. The large error bars originate from the corresponding low signal-to-noise ratio. The HWHM is almost constant at 1.5 and 4 meV for $T \leq 75$ K and starts to increase for $T \geq 100$ K at 4 meV. It is evident that there is a weak temperature dependence of the HWHM for $\omega \geq 6$ meV for all temperatures measured in this experiment. At these higher energies the HWHM increase almost linearly with temperature. In no case is the width in momentum space of the excitations appreciably affected by the superconducting transition.

The 2D integrated scattering function $S(\omega) = \int_{(\pi,\pi)} dq_{2D} S(\mathbf{q},\omega)$ and the 2D integrated susceptibility $\chi''(\omega) = \int_{(\pi,\pi)} dq_{2D} \chi''(\mathbf{q},\omega)$ can be obtained using the data discussed above. For $\omega \leq 4$ meV the scattering momentum width is almost independent of temperature for temperatures 1.9 K $\leq T \leq$ 75 K; thus the intensity at the $[\pi(1-\delta),\pi]$ position is simply proportional to the integrated scattering function and accordingly the maximum in the intensity at T_c still remains. On the other hand, we find that at 6 meV the integrated scattering intensity increases gradually with increasing temperature. For energies $\omega \leq 4$ meV, the integrated susceptibility shows the same behavior as a function of temperature up to 75 K as that shown in Fig. 4 of Ref. 10 for the peak

susceptibility. On the other hand, at 6 meV the susceptibility integrated around the (π,π) position is almost constant for $1.9\ \text{K} \leq T \leq 75\ \text{K}$.

We show in Fig. 5 the HWHM as a function of energy for $T=10$ and 35 K and energies $1.5\ \text{meV} \leq \omega \leq 20\ \text{meV}$. The HWHM is $0.034 \pm 0.006\ \text{Å}^{-1}$ at $\omega=1.5$ meV and

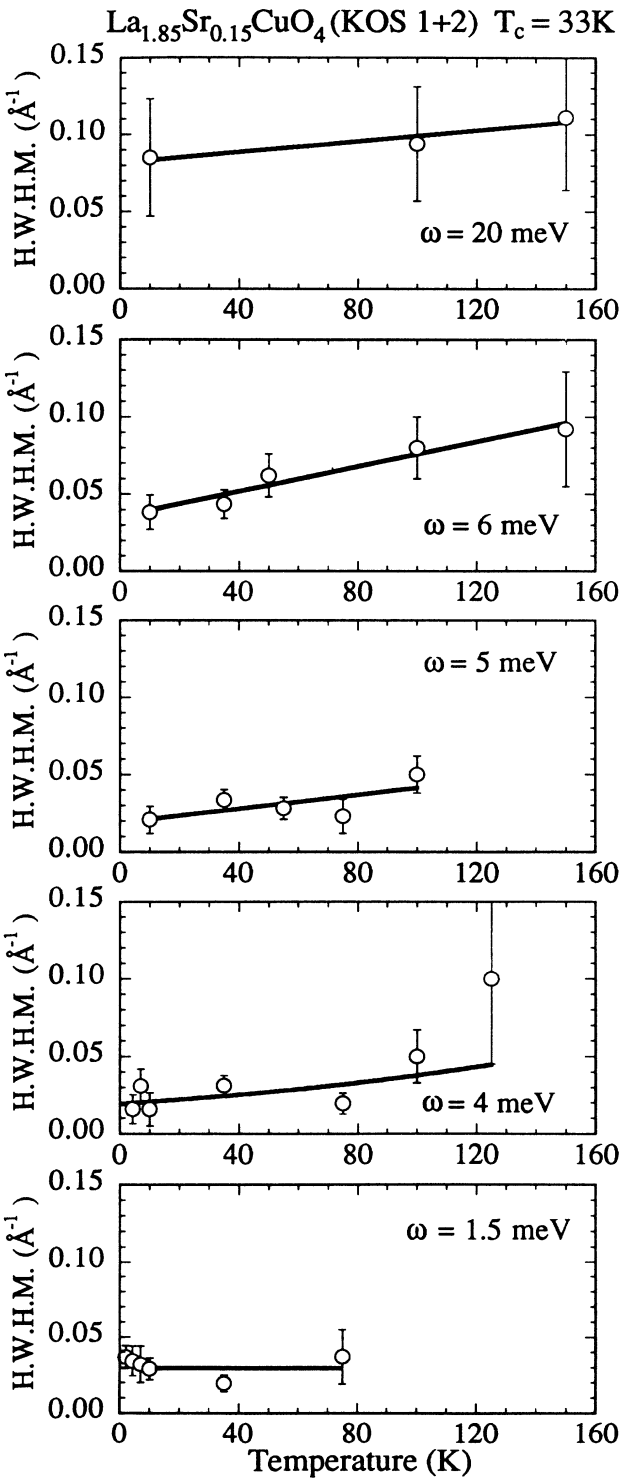

FIG. 4. Temperature dependences of the half width at half maximum of $S(\mathbf{q},\omega)$ in momentum space for energies of 1.5, 4, 5, 6, and 20 meV.

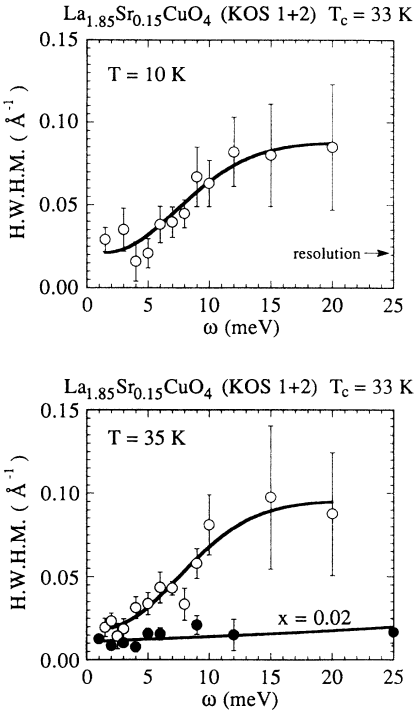

FIG. 5. Energy dependences of the half width at half maximum of $S(\mathbf{q},\omega)$ in momentum space for temperatures of 10 and 35 K for $La_{1.85}Sr_{0.15}CuO_4$ (open circles) and for $La_{1.98}Sr_{0.02}CuO_4$ (closed circles). The solid lines are guides to the eye.

$T=10$ K and increases by a factor of 4 between $\omega=1.5$ and 20 meV. The behavior is almost the same at $T=35$ K, which is just above T_c. Data for the $x=0.02$ sample at $T=35$ K are also shown in the lower panel of Fig. 5. These will be discussed in Sec. IV.

We show in Fig. 6 the integrated scattering function $S(\omega)$ as a function of energy for $T=10$ and 35 K and energies $1.5\ \text{meV} \leq \omega \leq 20\ \text{meV}$. The scattering function is almost constant for $\omega \geq 10$ meV and decreases below $\omega=10$ meV. It may be important that 10 meV is in fact the weak-coupling BCS gap energy as noted previously. There appears to be a minimum in the integrated intensity around an energy of 4 meV. At $T=35$ K the 10 meV pseudogap behavior still exists and the minimum in the integrated intensity at ~ 4 meV appears to be more pronounced.

From the data of Fig. 6 we extracted $\chi''(\omega)$ via the fluctuation-dissipation theorem. The results so obtained are shown in Fig. 7. Again there is the pseudogap behavior below 10 meV at $T=10$ and 35 K, while the 4-meV minimum behavior is less evident. In both Figs. 6 and 7 we show the corresponding data in $La_{1.98}Sr_{0.02}CuO_4$. Clearly, the energy dependence is quite different from that found in the superconducting samples. We shall discuss the significance of this difference in the next section.

The instantaneous structure factor $S(\mathbf{q})$ is obtained by integrating $S(\mathbf{q},\omega)$ over all energies. It is evident from Fig. 6 that the integral will be dominated by contributions from energies greater than ~ 10 meV where the

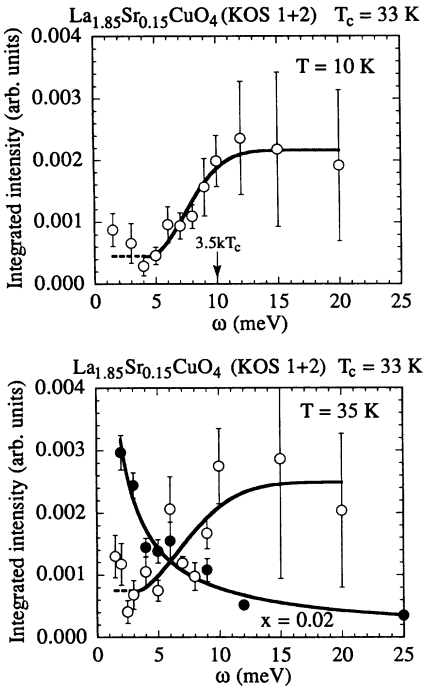

FIG. 6. Energy dependences of the 2D integrated scattering function $S(\omega)=\int_{(\pi,\pi)} dq_{2D} S(\mathbf{q},\omega)$ for temperatures of 10 and 35 K for $La_{1.85}Sr_{0.15}CuO_4$ (open circles) and for $La_{1.98}Sr_{0.02}CuO_4$ (closed circles). The data for the two samples have been scaled using phonon measurements so that this figure gives the correct relative intensities. The solid lines are guides to the eyes.

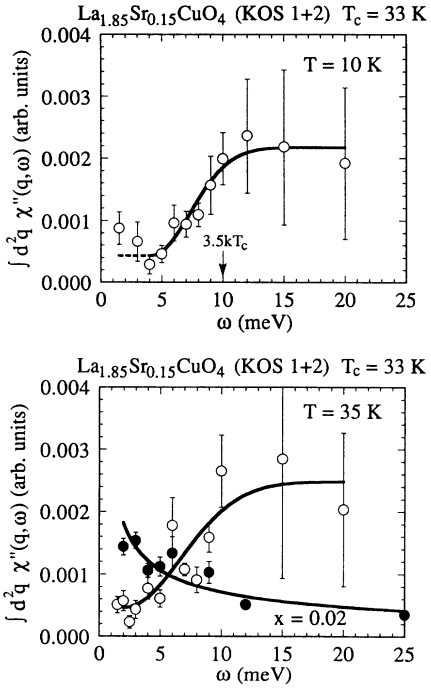

FIG. 7. Energy dependences of the 2D integrated susceptibility $\chi''(\omega)=\int_{(\pi,\pi)} dq_{2D}\chi''(\mathbf{q},\omega)$ for temperatures of 10 and 35 K for $La_{1.85}Sr_{0.15}CuO_4$ (open circles) and for $La_{1.98}Sr_{0.02}CuO_4$ (closed circles). The data for the two samples have been scaled using phonon measurements so that this figure gives the correct relative values. The solid lines are guides to the eye.

HWHM is ~ 0.08 Å^{-1}. Thus the correlation length in this sample is of order 12 Å, in agreement with earlier measurements on $La_{2-x}Sr_xCuO_4$ samples at Brookhaven.[1] This disagrees with the conclusions of Ref. 6 where the inverse correlation length is extracted from inelastic scans at low energies. The data in the two sets of experiments nevertheless agree reasonably well (see the Appendix).

IV. DISCUSSION

We first compare the current results with the previous measurements in Ref. 4. All the scans performed in Ref. 4 were taken in the untilted geometry in the $(h,0,l)$ configuration so that the observed intensity depended not only on the amplitude of the incommensurate magnetic peak but also on the peak width. It was found that the measured $S(\mathbf{q},\omega)$ exhibited a suppression below ~ 100 K for $\mathbf{q}$ near the (π,π) position in reciprocal space at $\omega=6$ meV, while at $\omega=12$ meV no such anomaly occurred. On the other hand, as shown here, $S(\mathbf{q},\omega)$ at the $[\pi(1-\delta),\pi]$ position at $\omega=6$ meV is almost independent of temperature. It is now clear that the diminution observed at 6 meV in Ref. 4 was in fact due to the decreasing width of the incommensurate peak as shown in Fig. 4. On the other hand, we find that $S(\mathbf{q},\omega)$ measured at the $[\pi(1-\delta,\pi)]$ position at $\omega=12$ meV decreases with increasing temperature, while the width increases with increasing temperature. This explains why $S(\mathbf{q},\omega)$ near the (π,π) position at 12 meV was found to be nearly constant as a function of temperature. Thus it now seems clear that the behavior observed in Ref. 4 was not simply connected to any superconducting pseudogap phenomenon appearing well above T_c, in contrast to suggestions made in that paper.

We now compare our results in $La_{1.85}Sr_{0.15}CuO_4$ with results in superconducting $YBa_2Cu_3O_{6.6}$ (Refs. 7–9) ($T_c=53$ K) as well as with those in $La_{1.98}Sr_{0.02}CuO_4$, a crystal with just enough Sr to destroy three-dimensional long-range magnetic order. The hole concentration in the $YBa_2Cu_3O_{6.6}$ sample[9] should be comparable to that in $La_{1.85}Sr_{0.15}CuO_6$ whereas, of course, the $x=0.02$ sample has of order 2% holes per Cu. First, the temperature dependence of $S(\mathbf{q},\omega)$ in $La_{1.85}Sr_{0.15}CuO_4$ is qualitatively similar to that observed by Sternlieb *et al.*[8] in $YBa_2Cu_3O_{6.6}$ albeit with the energy scale smaller by factor of ~ 1.8 which is, in fact, close to the ratio of the T_c's and there are also some minor differences in the behavior below T_c. Furthermore, above T_c the peak intensity data are qualitatively consistent with the ω/T scaling model developed by Keimer and co-workers[15,16] in their study of the spin fluctuations in nonsuperconducting and commensurate $La_{1.96}Sr_{0.04}CuO_4$; that is, χ'' increases with decreasing temperature at a rate which increases with decreasing energy. It should also be noted that in samples of $YBa_2Cu_3O_{6+x}$ with $T_c \geq 60$ K a gap appears below T_c which increases with increasing x and hence increasing hole concentration.[9] No such gap is found in $La_{1.85}Sr_{0.15}CuO_4$.

We show in Fig. 5 the HWHM as a function of energy for $T=35$ K and energies 1 meV $\leq\omega\leq$ 25 meV in

$La_{1.98}Sr_{0.02}CuO_4$. Note that the scattering is commensurate in this sample. The HWHM is 0.02 ± 0.003 Å^{-1} at $\omega=1$ meV and $T=10$ K. This width is quite close to that measured in $La_{1.85}Sr_{0.15}CuO_4$ at low energies. In $La_{1.98}Sr_{0.02}CuO_4$ the energy dependence of the width is quite moderate with the width increasing by at most a factor of 1.5 between $\omega=1$ meV and 25 meV. We should note that the quantitative value of the deconvoluted width depends on what function is used for the cross section. We used 2D Lorentzian profiles in the fits. As mentioned in Sec. III, 2D squared Lorentzian profiles give widths broader by a factor of ~1.4 at low energies and ~1.1 at high energies compared with the results of fits to 2D Lorentzian profiles. This is because the resolution function is much coarser along the direction perpendicular to the scattering plane than the intrinsic scattering width, and consequently the integration along the vertical direction affects the observed width in the scattering plane. In nonsuperconducting $La_{2-x}Sr_xCuO_4$,[15,16] a 2D Lorentzian profile was used as the cross section for $S(\mathbf{q})$. It was found in Ref. 16 for $x=0.04$ that the inelastic scattering widths for energies $1\le\omega\le12$ meV corresponded well to the inverse correlation length determined by two-axis (energy-integrating) measurements. Because of that, 2D Lorentzian profiles have also been used in this study. Therefore, the widths and the intensities presented in this paper are correct relative to each other, but their absolute values may have some ambiguity. We should note that we have also carried out a complete data analysis using Lorentzian squared profiles and none of the essential conclusions in this paper are changed.

In $YBa_2Cu_3O_{6.6}$ (Refs. 7 and 8) the scattering is nearly commensurate at the (π,π) position and the scattering momentum width is almost temperature independent for temperatures 10 K $\le T\le$ 100 K. The difference in the geometry of the spin fluctuations in $La_{1.85}Sr_{0.15}CuO_4$ and $YBa_2Cu_3CuO_{6.6}$ is believed to arise from differences in the Fermi surfaces.[12] The widths of the scans in q space in $YBa_2Cu_3O_{6.6}$ at $T=10$ K are 0.10 Å^{-1} for $\omega=5$ meV and 0.13 Å^{-1} for $\omega=18$ meV. The width at 18 meV is similar to the values we measure in $La_{1.85}Sr_{0.15}CuO_4$, but at low energies the width measured in $YBa_2Cu_3O_{6.6}$ is a factor of 3 larger than that of $La_{1.85}Sr_{0.15}CuO_4$. Generally, various calculations including especially those by Levin and co-workers[12] based on a nearly localized Fermi-liquid model seem to account very well overall for the measured spin-fluctuation spectra in both $La_{1.85}Sr_{0.15}CuO_4$ and $YBa_2Cu_3O_{6.6}$ in the normal state including the temperature and energy dependences. These theories have not, however, yet addressed the marked sharpening of the HWHM at low energies which we observe for temperatures below ~75 K in $La_{1.85}Sr_{0.15}CuO_4$.

The energy dependences of the integrated intensity $S(\omega)=\int dq_{2D}S(\mathbf{q},\omega)$ and the integrated susceptibility $\chi''(\omega)\overset{(\pi,\pi)}{=}\int_{(\pi,\pi)}dq_{2D}\chi''(\mathbf{q},\omega)$, for $La_{1.98}Sr_{0.02}CuO_4$ are compared with those for $La_{1.85}Sr_{0.15}CuO_4$ in Figs. 6 and 7, respectively. The data for the two samples have been scaled by the relative volumes, which were determined by phonon measurements. The integrated scattering intensity as well as the integrated susceptibility for the 2% sample decrease with increasing energy in agreement with earlier measurements.[14–16] This behavior is quite different from that of $La_{1.85}Sr_{0.15}CuO_4$, in which a pseudogap exists. Specifically, as noted above, in the superconducting sample the integrated scattering function as well as the integrated susceptibility are almost constant above $\omega\sim10$ meV and then begin to decrease with decreasing ω at $\omega\sim10$ meV, which corresponds to the weak-coupling BCS superconducting gap energy $2\Delta=3.5kT_c$. In $YBa_2Cu_3O_{6.6}$ the pseudogap behavior is more pronounced and the intensities below 5 meV are near zero, although strong magnetic scattering is observed well below $2\Delta(\sim18$ meV). It should be emphasized that the pseudogap behavior in the integrated response function in $La_{1.85}Sr_{0.15}CuO_4$ originates primarily from the energy dependence of the scattering momentum width because the 2D integrated intensity depends on the square of the width. On the other hand, in $YBa_2Cu_3O_{6.6}$ the observed gaplike behavior mostly originates from the energy dependence of the amplitude. It is also important to note that in $YBa_2Cu_3O_{6.6}$ doping with sufficient Zn to destroy superconductivity[21] converts the ω dependence of $\chi''(\omega)$ to the form observed in $La_{2-x}Sr_xCuO_4$ for $x=0.02$ and 0.04.

Perhaps the most surprising feature of Figs. 6 and 7 is that for energies above ~10 meV the q-integrated susceptibility $\chi''(\omega)$ in $La_{1.85}Sr_{0.15}CuO_4$ is about a factor of 3 larger than that in $La_{1.98}Sr_{0.02}CuO_4$ at the same energies. The latter in turn should be comparable to the spin-wave value for $\chi''(\omega)$ in the pure material La_2CuO_4. This enhancement of the integrated susceptibility above that characterizing the lightly doped system is to us a very surprising result. We should note that exactly the same enhancement effect has recently been observed[19] in $YBa_2Cu_3O_{6.6}$ ($T_c=53$ K) compared with $YBa_2Cu_3O_{6.15}$ ($T_N=415$ K) albeit at an energy scale a factor of ~1.8 (the ratio of the T_c's) larger than that in $La_{1.85}Sr_{0.15}CuO_4$. Once more, the similarities in the energy and temperature dependence of $\chi''(\mathbf{q},\omega)$ in $La_{1.85}Sr_{0.15}CuO_4$ ($T_c=33$ K) and $YBa_2Cu_3O_{6.6}$ ($T_c=53$ K) are striking. These two materials have comparable hole densities but very different Fermi surfaces and, as noted above, somewhat different geometries for $\chi''(\mathbf{q},\omega)$, the former being incommensurate and the latter commensurate at (π,π).

As mentioned in Sec. III, since the line shape for $\omega\le4$ meV is independent of temperature below ~75 K, $\chi''(\mathbf{q},\omega)$ at the $[\pi(1-\delta),\pi]$ position is directly proportional to the 2D integrated susceptibility $\chi''(\omega)$ in this energy range. We now compare this with nuclear quadrupole resonance (NQR) measurements[17,18] of $(T_1T)^{-1}$ at the copper site, which is proportional to an integral of $\chi''(\mathbf{q},\omega)$ over $\mathbf{q}$, weighted by form factors, with $\omega\to0$. $(T_1T)^{-1}$ shows a maximum somewhat above T_c and then decreases gradually to zero with further decrease in temperature. As noted in Ref. 10 this behavior is rather different from that of our neutron data at $\omega=1.5$ meV. Clearly, further theory is required to relate our measured $\chi''(\mathbf{q},\omega)$ at nonzero ω to that inferred for the $\omega\to0$ limit from the NQR data. This difference also illustrates the danger in generalizing $\omega\to0$ results for $\chi''(q,\omega)$ to the

higher energies relevant for superconductivity.

Theoretical calculations[11,12] of $\chi''(\mathbf{q},\omega)$ with conventional S-wave BCS models predict that the spectral weight for $\omega < 2\Delta$, where Δ is the superconducting gap, observed near $[\pi(1-\delta),\pi]$ should be rapidly suppressed to zero as T drops below T_c. However, the spectral weight for a $d_{x^2-y^2}$ wave gap can remain significant for $T < T_c$. As shown in Fig. 3 we observe strong magnetic scattering well below the weak-coupling gap energy. It is also predicted by some theoretical calculations[12] that for a $d_{x^2-y^2}$ superconducting wave function the geometry of $\chi''(q,\omega)$ should change below T_c, and specifically new peaks at the $[\pi(1\pm\delta),\pi(1\pm\delta)]$ and $[\pi(1\pm\delta),\pi(1\pm\delta)]$ positions should become dominant at low temperatures. However, as reported first in Ref. 22 for $La_{1.85}Sr_{0.15}Cu_{0.988}Zn_{0.012}O_4$ ($T_c = 16$ K) this component is unobservable within statistical error even at 1.9 K for 1.5 meV $\leq T \leq$ 4 meV. A similar result was obtained down to 10 K by Thurston *et al.*[10] in $La_{1.85}Sr_{0.15}CuO_4$. Consistent with these results we find that in $La_{1.85}Sr_{0.15}CuO_4$ at these energies the line shapes and positions of the incommensurate peaks are nearly independent of temperature below T_c down to 1.9 K (cf. Fig. 3). Thus it appears, in agreement with Ref. 22, that the simplest $d_{x^2-y^2}$ model for the superconductivity cannot be correct. This conundrum may, however, be resolved by inclusion of the effects of disorder.

In summary, we have studied the temperature and energy dependence of the incommensurate magnetic scattering of $La_{1.85}Sr_{0.15}CuO_4$. The width of $S(\mathbf{q},\omega)$ in momentum space increases with increasing temperature and/or energy. The q width becomes remarkably sharp at low ω and at low temperatures, where the measured values are a factor of 3 smaller than those found in $YBa_2Cu_3O_{6.6}$;[7,8] indeed the low-energy momentum widths are close to those found in $La_{1.98}Sr_{0.02}CuO_4$. The integrated susceptibility $\chi''(\omega)$ shows a pseudogap behavior for energies ≤ 10 meV at low temperatures although nonzero intensity is observed below T_c down to 1.9 K. This behavior is qualitatively similar to that found in $YBa_2Cu_3O_{6.6}$.[7,8] The behavior is, however, quite different from that found in nonsuperconducting samples such as $La_{1.98}Sr_{0.02}CuO_4$, where the integrated scattering function is a constant over a wide range of energies and then increases with decreasing energy at low energies. Surprisingly, $\chi''(\omega)$ is enhanced by a factor of ~ 3 at intermediate energies in the superconductor compared with the pure/lightly doped materials. Clearly, these results should provide both guidance and a testing ground for any models of the magnetism and the superconductivity in the lamellar copper-oxide superconductors.

ACKNOWLEDGMENTS

We would like to thank G. Aeppli, V. J. Emery, P. A. Lee, K. Levin, D. J. Scalapino, B. J. Sternlieb, and J. M. Tranquada for helpful discussions. This work was supported by the U.S.-Japan Cooperative Neutron-Scattering Program. The work at Tohoku University was supported by a Grant-In-Aid for Scientific Research for the Japanese Ministry of Education, Science and Culture. The work at BNL was supported by the Division of Materials Science, the Office of Basic Energy Science of the U.S. Department of Energy, under Contract No. DE-AC02-76CH00016. The work at MIT was supported by the U.S. National Science Foundation under Contracts No. DMR 90-22933 and DMR 90-07825.

APPENDIX

Mason *et al.*[23] recently reported neutron-scattering measurements in superconducting $La_{1.86}Sr_{0.14}CuO_4$ ($T_c = 35$ K) and heat-capacity measurements in a small single crystal of $La_{1.86}Sr_{0.14}CuO_4$. The heat-capacity measurements reveal a residual contribution to C/T at low temperatures corresponding to a constant density of states near zero energy; this supports strongly the assertion by Thurston *et al.*[10] that this system exhibits other than simple S-wave BCS superconductivity.

The neutron-scattering measurements of Ref. 23 parallel our own and those of Ref. 10, albeit with somewhat worse signal to background. Their results agree with ours in detail. We show in Fig. 8 the data of Mason *et al.*[23] for $\chi''(\mathbf{q},\omega)$ of the $[\pi(1-\delta),\pi]$ position as a function of temperature for energies of 6, 3.5, and 1.2 meV superimposed on our data at energies of 6, 3, and 1.5 meV. The relative amplitudes have been chosen to give the best overall agreement. It is evident that the temperature dependences exhibited in the two sets of data agree to within the combined experimental errors. There may, however, be a subtle difference in the energy dependence of $\chi''(\omega)$ at the lowest energies; establishing such a difference will require comparison of actual data for the

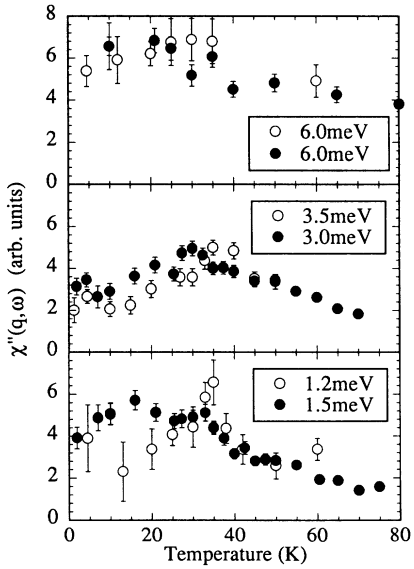

FIG. 8. Temperature dependence of $\chi''(\mathbf{q},\omega)$ at the position $[\pi(1-\delta),\pi]$ as measured by ourselves in $La_{1.85}Sr_{0.15}CuO_4$ ($T_c = 33$ K) and Mason *et al.* (Ref. 23) in $La_{1.86}Sr_{0.14}CuO_4$ ($T_c = 35$ K). The closed circles are our data whereas the open circles are those of Mason *et al.* (Ref. 23).

two samples taken under identical conditions. As noted previously, the widths of scans in **q** at various energies measured by Mason *et al.*[23] also agree with our own results. They also corroborate our result and that of Ref. 22 that the geometry of $\chi''(\mathbf{q},\omega)$ is not affected by the superconductivity for temperatures well below T_c. This overall agreement verifies the universality and fundamental nature of our observations in $La_{1.85}Sr_{0.15}CuO_4$.

---

*Present address: RIKEN: The Institute of Physical & Chemical Research, Wako, Saitama 351-01, Japan.

[1]R. J. Birgeneau, D. R. Gabbe, H. P. Jenssen, M. A. Kastner, P. J. Picone, T. R. Thurston, G. Shirane, Y. Endoh, M. Sato, K. Yamada, Y. Hidaka, M. Oda, Y. Enomoto, M. Suzuki, and T. Murakami, Phys. Rev. B **38**, 6614 (1988); For a review of early work, see R. J. Birgeneau and G. Shirane, in *Physical Properties of High-Temperature Superconductors I,* edited by D. M. Ginsberg (World Scientific, Singapore, 1989), p. 151.

[2]H. Yoshizawa, S. Mitsuda, H. Kitazawa, and K. Katsumata, J. Phys. Soc. Jpn. **57**, 3686 (1988); R. J. Birgeneau, Y. Endoh, Y. Hidaka, K. Kakurai, M. A. Kastner, T. Murakami, G. Shirane, T. R. Thurston, and K. Yamada, Phys. Rev. B **39**, 2868 (1989).

[3]T. R. Thurston, R. J. Birgeneau, M. A. Kastner, N. W. Preyer, G. Shirane, Y. Fujii, K. Yamada, Y. Endoh, K. Kakurai, M. Matsuda, Y. Hidaka, and T. Murakami, Phys. Rev. B **40**, 4585 (1989).

[4]G. Shirane, R. J. Birgeneau, Y. Endoh, P. Gehring, M. A. Kastner, K. Kitazawa, H. Kojima, I. Tanaka, T. R. Thurston, and K. Yamada, Phys. Rev. Lett. **63**, 330 (1989).

[5]S.-W. Cheong, G. Aeppli, T. E. Mason, H. A. Mook, S. M. Hayden, P. C. Canfield, Z. Fisk, K. N. Clausen, and J. L. Martinez, Phys. Rev. Lett. **67**, 1791 (1991).

[6]T. E. Mason, G. Aeppli, and H. A. Mook, Phys. Rev. Lett. **68**, 1414 (1992).

[7]J. M. Tranquada, P. M. Gehring, G. Shirane, S. Shamoto, and M. Sato, Phys. Rev. B **46**, 5561 (1992).

[8]B. J. Sternlieb, G. Shirane, J. M. Tranquada, M. Sato, and S. Shamoto, Phys. Rev. B **67**, 5320 (1993).

[9]J. Rossat-Mignod, L. P. Regnault, C. Vettier, P. Bourges, P. Burlet, J. Bossy, J. Y. Henry, and G. Lapertet, Physica B **180-181**, 383 (1992); for a recent review, see J. Rossat-Mignod, L. P. Regnault, P. Bourges, P. Burlet, C. Vettier, and J. Y. Henry, in *Frontiers in Solid State Sciences I,* edited by L. C. Gupta and M. S. Multani (World Scientific, Singapore, 1992), p. 265.

[10]T. R. Thurston, P. M. Gehring, G. Shirane, R. J. Birgeneau, M. A. Kastner, Y. Endoh, M. Matsuda, K. Yamada, H. Kojima, and I. Tanaka, Phys. Rev. B **46**, 9128 (1992).

[11]See, for example, N. Bulut and D. J. Scalapino, Phys. Rev. Lett. **68**, 706 (1991); Phys. Rev. B **45**, 2371 (1992); **47**, 3419 (1993); J. Ruvalds, C. Rieck, J. Zhang, and A. Virocztek, Science **256**, 1667 (1992); P. Benard, L. Chen, and A.-M. S. Tremblay, Phys. Rev. B **47**, 589 (1993); P. B. Littlewood, J. Zaanen, G. Aeppli, and H. Monien, *ibid.* **48**, 487 (1993); P. Monthoux and D. Pines, *ibid.* **47**, 6067 (1993); D. Thelen, D. Pines, and J. P. Lu, Phys. Rev. **47**, 9151 (1993); For an alternative approach based on frustrated phase separation see V. J. Emery and S. A. Kivelson, Physica C **209**, 597 (1993).

[12]Q. Si, Y. Zha, K. Levin, and J. P. Lu, Phys. Rev. B **47**, 9055 (1993); Y. Zha, K. Levin, and Q. Si, *ibid.* **47**, 9124 (1993); Y. Zha, Q. M. Si, and K. Levin, Physica C **212**, 413 (1993); T. Tanomoto, H. Kohno, and H. Fukuyama, J. Phys. Soc. Jpn. **62**, 1455 (1993).

[13]I. Tanaka and H. Kojima, Nature (London) **337**, 21 (1989).

[14]M. Matsuda, R. J. Birgeneau, Y. Endoh, Y. Hidaka, M. A. Kastner, K. Nakajima, G. Shirane, T. R. Thurston, and K. Yamada, J. Phys. Soc. Jpn. **62**, 1702 (1993).

[15]B. Keimer, R. J. Birgeneau, A. Cassanho, Y. Endoh, R. W. Erwin, M. A. Kastner, and G. Shirane, Phys. Rev. Lett. **67**, 1930 (1991).

[16]B. Keimer, N. Belk, R. J. Birgeneau, A. Cassanho, C. Y. Chen, M. Greven, M. A. Kastner, A. Aharony, Y. Endoh, R. W. Erwin, and G. Shirane, Phys. Rev. B **46**, 14 034 (1992).

[17]Y. Kitaoka, S. Ohsugi, K. Ishida, and K. Asayama, Physica C **170**, 189 (1990).

[18]S. Ohsugi, Y. Kitaoka, K. Ishida, and K. Asyama, J. Phys. Soc. Jpn. **60**, 2351 (1991).

[19]Y. Endoh, K. Yamada, M. Matsuda, K. Nakajima, K. Kuroda, Y. Hidaka, I. Tanaka, H. Kojima, R. J. Birgeneau, M. A. Kastner, B. Keimer, G. Shirane, and T. R. Thurston, Jpn. J. Appl. Phys. **7**, 174 (1992).

[20]S. Shamoto, M. Sato, J. M. Tranquada, B. J. Sternlieb, and G. Shirane, Phys. Rev. B **48**, 13 817 (1993).

[21]K. Kakurai, S. Shamoto, T. Kiyokura, M. Sato, J. M. Tranquada, and G. Shirane, Phys. Rev. B **48**, 3485 (1993).

[22]M. Matsuda, R. J. Birgeneau, H. Chou, Y. Endoh, M. A. Kastner, H. Kojima, K. Kuroda, G. Shirane, I. Tanaka, and K. Yamada, J. Phys. Soc. Jpn. **62**, 443 (1993).

[23]T. E. Mason, G. Aeppli, S. M. Hayden, A. P. Ramirez, and H. A. Mook, Phys. Rev. Lett. **71**, 919 (1993).